Pramana – J. Phys. (2018) 91:74
https://doi.org/10.1007/s12043-018-1646-6

Lasing without population inversion in a four-level Y-type configuration in double quantum dot system

B AL-NASHY[1,*], M ABDULLAH[2], ALI GEHAD AL-SHATRAVI[3] and AMIN HABBEB AL-KHURSAN[2]

[1]Science College, Misan University, Amarah, Misan, Iraq
[2]Nassiriya Nanotechnology Research Laboratory (NNRL), Science College, Thi-Qar University, Nassiriya, Dhi Qar, Iraq
[3]Physics Department, Science College, Thi-Qar University, Nassiriya, Dhi Qar, Iraq
*Corresponding author. E-mail: baq_o@yahoo.com

MS received 13 February 2018; revised 18 April 2018; accepted 25 April 2018; published online 24 September 2018

Abstract. This work discusses lasing without inversion in Y-scheme in a double quantum dot nanostructure. This new type of lasing, which results from the quantum interference of spontaneous emission components, was not discussed earlier in quantum dot nanostructures. It is found that both pumping and cycling fields control the laser emission. The decrease of the cycling detuning increases the possibility of lasing. Probe detuning controls the width of the absorption bath (electromagnetic-induced transparency window) of this structure. This phenomenon can have an interesting application for developing sources of coherent radiation in a region of electromagnetic spectrum where the implementation of traditional laser schemes is difficult.

Keywords. Double quantum dot; Y-structure; lasing without inversion.

PACS Nos 42.55.Px; 78.67.Hc; 32.80.Xx

1. Introduction

Quantum dots (QDs) are nanoscale crystals in which the states are quantised in all dimensions. In a semiconductor QD, the confined electronic states can be accurately controlled by varying the dot size, shape or composition [1]. For example, the band gap in a QD, which determines the frequency range of the emitted light, is inversely related to its size. In fluorescent dye applications, the frequency of emitted light increases as the size of the QD decreases. Consequently, the colour of the emitted light changes from red to blue when the size of the QD is made smaller. This allows the excitation and emission of QDs to be highly tunable [2].

Many interesting phenomena in optics such as quantum beats and self-induced transparency originate from the atomic coherence and interference of radiative processes. Under special conditions, coherent atomic transitions can cancel absorption. The resulted atomic coherence was used in coherent trapping, electromagnetically-induced transparency (EIT), enhancement of the index of refraction in the non-absorbing media and lasing without inversion (LWI) [3].

LWI is a technique used for light amplification by stimulated emission without the requirement of population inversion [4]. A laser work under this scheme exploits the quantum interference between the probability amplitudes of atomic transitions in order to eliminate absorption without disturbing the stimulated emission [5].

The cancellation of absorption provides the possibility to obtain light amplification even if the population of the upper level is less than that of the lower level, which is the main idea of the LWI. Such a situation can be realised, for instance, in a three-level system when two coherent atomic transitions destructively interfere and, hence, cancel absorption. This phenomenon has an interesting application for developing the sources of coherent radiation in a region of electromagnetic spectrum where the implementation of traditional laser schemes is either too difficult or impractical [3].

Three-level systems such as Λ-type and V-type can be used to obtain the LWI. Quantum interference, induced by coherent fields, results from the three-level systems and exhibits novel light amplification phenomena which are different from that of the two-level systems. For

example, multilevel systems which create laser gain at frequencies far removed from that of the coherent coupling fields, provide possibilities for the generation of coherent radiation in the short-wavelength regime. Furthermore, there are novel statistical properties such as reduced laser linewidth [1].

In general, LWI can be classified into two categories: first, LWI in any state basis and second, LWI in the bare atomic states, but with inversion in a hidden-state basis such as dressed states [6]. In the latter case, when the coupling field is detuned from the atomic transition, there is an inversion in dressed states which is accounted for light amplification, but this is limited to the condition that the coupling field is far stronger than the probe field. When the probe field is comparable to the coupling field, there is still LWI which cannot be attributed to the inversion in the dressed states [7].

The origin of LWI is the gain at the emission peak. Gain without inversion has been realised in many systems such as atomic systems, semiconductor nanostructures and molecules [8,9].

Due to the possibility of fabricating a double quantum dot (DQD) system using self-assembled growth technology [10], the optical properties of the DQD was a subject of study for many groups. For example, Villas-Boas *et al* [10] studied the possibility of controlling the optical properties of the DQD system by accessing Rabi oscillations. Mahmoudi and Sahrai [11] studied superluminal and subluminal light propagation in the DQD system.

The DQD system in the Y-configuration was proposed in [12,13] for high nonlinearity purposes. In this work, we are going to investigate the LWI in a four-level Y-type configuration in the DQD system. The aim of this work is to put Rabi frequency under control for attaining gain without inversion. It is shown that probe detuning plays an essential role in this work. It is also shown that one can use the pumping field to switch between absorption and gain.

2. The proposed QD structure

The proposed structure used to simulate the DQD system is shown in figure 1, which is an asymmetric InAs DQD with 4 nm height and 10 nm width for the left dot and 2 nm height and 14 nm width for the right dot. Their ground and excited conduction energy subbands are 0.8 and 1.07 eV for the left QD and 0.91 and 1.05 eV for the right one [12]. This structure can be obtained by the self-assemble growth technique [14]. The ground state (GS) for the left dot is the $|0\rangle$ state of the system, the GS and ES of the right dot are the states $|1\rangle$ and $|2\rangle$ and the state $|3\rangle$ is the ES of the left dot.

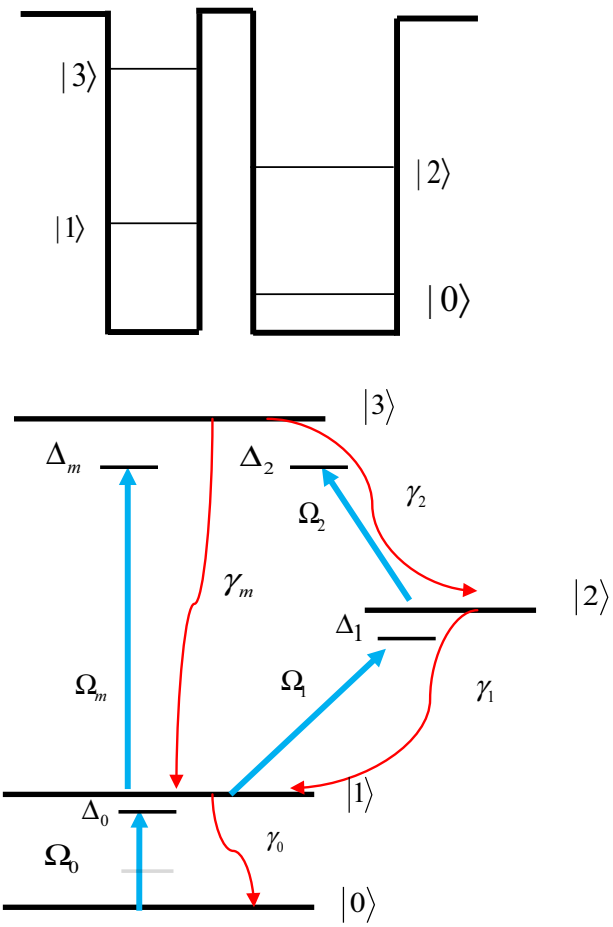

Figure 1. Schematic energy level diagram of a four-level system in Y-configuration. Here, $\omega_0(\Delta_0)$, $\omega_1(\Delta_1)$, $\omega_2(\Delta_2)$ and $\omega_m(\Delta_m)$ are frequencies (frequency detunings) of the probe, cycling, coupling and pumping fields, respectively [9].

3. Y-type model in DQD nanostructures

Consider a four-level Y-type configuration in the DQD system. This can be obtained in a QD molecule with two conduction sub-band levels for each one [13], as shown in figure 1a. The intersub-band transitions can be easily realised experimentally [10]. Sub-band configurations have two subsystems. For the first subsystem, the subbands are considered as $|0\rangle$, $|1\rangle$, $|2\rangle$ and $|3\rangle$ forming a Λ-type subsystem with the $|0\rangle \rightarrow |1\rangle$ transition with an energy $\hbar\omega_{10}$. It is driven by a weak probe field E_0 of frequency ω_0 with Rabi frequency $\Omega_0 = E_0 d_{10}/\hbar$. The $|1\rangle \rightarrow |2\rangle$ transition with $\hbar\omega_{21}$ energy is due to the strong cycling field E_1, frequency ω_1 and Rabi frequency $\Omega_1 = E_1 d_{21}/\hbar$. The $|2\rangle \rightarrow |3\rangle$ transition with $\hbar\omega_{32}$ energy is due to the coupling field E_2, frequency ω_2 and Rabi frequency $\Omega_2 = E_2 d_{32}/\hbar$. The second subsystem contains $|0\rangle$, $|1\rangle$ and $|3\rangle$ subbands, which form a ladder-type system where the $|1\rangle \rightarrow |3\rangle$ transition with $\hbar w_{13}$ energy is due to the strong pump field E_3.

The corresponding detunings for these transitions are: $\Delta_2 = \omega_2 - \omega_{23}$, $\Delta_m = \omega_m - \omega_{13}$, $\Delta_1 = \omega_1 - \omega_{12}$ and $\Delta_0 = \omega_0 - \omega_{01}$. The two middle levels $|1\rangle$ and $|2\rangle$, upper level $|3\rangle$ and the ground level $|0\rangle$ form a closed interaction contour. The phases associated with the four coherent fields E_0, E_1, E_2 and E_m are ϕ_0, ϕ_1, ϕ_2 and ϕ_m, respectively. Driving transitions between double dots by laser fields were examined in a number of works [15,16]. Using the density matrix approach, we can write the following dynamical equations for our system (see figure 1b):

$$
\begin{aligned}
\dot{\rho}_{00} &= \gamma_0\rho_{11} + \mathrm{i}\Omega_0(\rho_{10} - \rho_{01}),\\
\dot{\rho}_{11} &= -(\gamma_0\rho_{11} + \gamma_1\rho_{22} + \gamma_3\rho_{33}) + \mathrm{i}[\Omega_0(\rho_{10} - \rho_{10})\\
&\quad + \Omega_1(\rho_{21} - \rho_{12}) + \Omega_m(\rho_{31} - \rho_{13})],\\
\dot{\rho}_{11} &= -(\gamma_0\rho_{11} + \gamma_1\rho_{22} + \gamma_3\rho_{33}) + \mathrm{i}[\Omega_0(\rho_{10} - \rho_{10})\\
&\quad + \Omega_1(\rho_{21} - \rho_{12}) + \Omega_m(\rho_{31} - \rho_{13})],\\
\dot{\rho}_{22} &= -(\gamma_1\rho_{22} + \gamma_2\rho_{33}) + \mathrm{i}[\Omega_1(\rho_{12} - \rho_{21})\\
&\quad + \Omega_2(\rho_{32} - \rho_{23})],\\
\dot{\rho}_{33} &= -(\gamma_2 + \gamma_3)\rho_{33} + \mathrm{i}[\Omega_m(\rho_{13} - \rho_{31})\\
&\quad + \Omega_2(\rho_{23} - \rho_{32})],\\
\dot{\rho}_{10} &= -(\mathrm{i}\Delta_0 + \gamma_0)\rho_{10} + \mathrm{i}[\Omega_0(\rho_{00} - \rho_{11})\\
&\quad + \Omega_1\rho_{20}\mathrm{e}^{\mathrm{i}\varphi} + \Omega_m\rho_{30}],\\
\dot{\rho}_{20} &= \left[-\mathrm{i}(\Delta_0 + \Delta_1) - (\gamma_0 + \gamma_1)\right]\rho_{20}\\
&\quad + \mathrm{i}[\Omega_1\rho_{10}\mathrm{e}^{\mathrm{i}\Phi} + \Omega_2\rho_{30} - \Omega_0\rho_{21}\mathrm{e}^{\mathrm{i}\Phi}],\\
\dot{\rho}_{30} &= \left[-\mathrm{i}(\Delta_0 + \Delta_m) - (\gamma_0 + \gamma_2 + \gamma_3)\right]\rho_{30}\\
&\quad + \mathrm{i}[\Omega_m\rho_{10} + \Omega_2\rho_{20} - \Omega_0\rho_{31}],\\
\dot{\rho}_{12} &= -[\mathrm{i}\Delta_0 + \mathrm{i}\Delta_1 + \gamma_1]\rho_{12} + \mathrm{i}[\Omega_0\rho_{02}\mathrm{e}^{\mathrm{i}\varphi}\\
&\quad + \Omega_1(\rho_{22} - \rho_{11}) + \Omega_m\rho_{32}\mathrm{e}^{\mathrm{i}\varphi} - \Omega_2\rho_{13}\mathrm{e}^{\mathrm{i}\varphi}],\\
\dot{\rho}_{13} &= -(\mathrm{i}\Delta_m + \gamma_2 + \gamma_3)\rho_{13} + \mathrm{i}[\Omega_m(\rho_{33} - \rho_{11})\\
&\quad + \Omega_0\rho_{03} + \Omega_1\rho_{23} - \Omega_2\rho_{12}\mathrm{e}^{\mathrm{i}\varphi}],\\
\dot{\rho}_{23} &= \left[-\mathrm{i}(\Delta_0 + \Delta_1 + \Delta_2) - (\gamma_2 + \gamma_3)\right]\rho_{23}\\
&\quad + \mathrm{i}[\Omega_2(\rho_{33} - \rho_{22}) + \Omega_1\rho_{13} - \Omega_m\rho_{21}\mathrm{e}^{\mathrm{i}\varphi}].
\end{aligned}
$$

Then the linear first-order susceptibility is given by [17,18]

$$\chi^{(1)} = \frac{2N\mu_{10}^2}{\varepsilon_0\hbar\Omega_0}\rho_{10}^{(1)},$$

where N is the atomic number density in the medium. The real and imaginary parts of $\chi^{(1)}$ correspond to the linear dispersion and absorption, respectively. ε_0 is the permittivity of free space, $\hbar$ is the normalised Planks constant, $\rho_{10}^{(1)}$ is the first order of the density operator of the probe transition and Ω_0 is the Rabi frequency of the probe field.

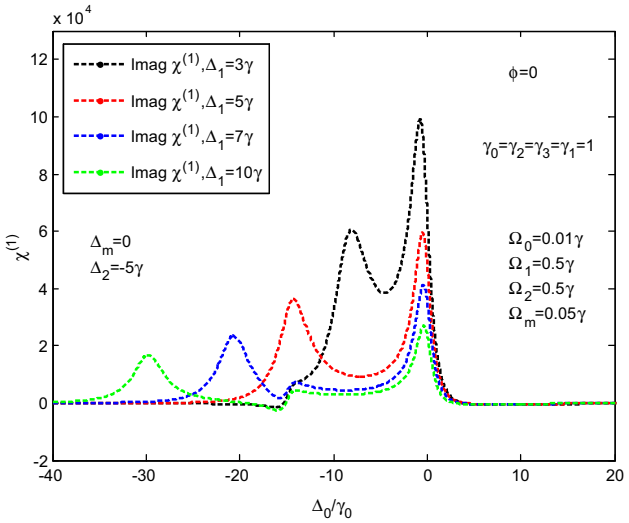

Figure 2. Linear susceptibility as a function of normalised probe detuning Δ_0/γ_0 at different cycling detunings Δ_1.

4. Results and discussion

The assumption of identical relaxation was used here ($\gamma_0 = \gamma_1 = \gamma_2 = \gamma_3 = 1$ meV) to simplify the calculations. This assumption was also used in a large number of works, e.g. in [17] for the atomic system, in [19] for the quantum well system and in [20] for the QD system. To identify LWI, the first-order nonlinear susceptibility was plotted in all the following figures.

Figure 2 shows the first-order nonlinear susceptibility as a function of normalised probe detuning Δ_0/γ_0 for the DQD system. The following parameters are considered: $\Delta_2 = -5\gamma$ and $\Delta_m = 0$, probe, pump, cycling and coupling, Rabi optical frequencies are, respectively, $\Delta_2 = -5\gamma$, $\Omega_1 = \Omega_2 = 0.5\gamma$ and $\Omega_m = 0.05\gamma$, with cycling detuning Δ_1 as a variable parameter. It shows an increase in the absorption with the reduction of cycling field detuning. The absorption peaks appear at negative probe detuning, showing the effect of negative coupling field detuning Δ_2. There is no occurrence of lasing.

Figure 3 shows the effect of pumping field Ω_m on absorption under the following detuning: $\Delta_1 = 0$, $\Delta_2 = \Delta_m = 3\gamma$, and Rabi frequencies $\Omega_0 = 0.01\gamma$, $\Omega_1 = 0.03\gamma$ and $\Omega_2 = 0.3\gamma$. When $\Omega_m = 0.01\gamma$ and 0.03γ, only absorption appears (black and red curves, respectively). Increasing Ω_m to 0.3γ changes the absorption into a gain with the appearance of the EIT window. Increasing the pump field to $\Omega_m = 0.7\gamma$ removes the EIT window and gives high gain. This result coincides with the conclusion in [21], where the EIT window is shown at low power.

Figure 4 shows linear susceptibility as a function of cycling field Ω_1 with probe detuning (Δ_0) as a variable parameter, which examines the controllability of

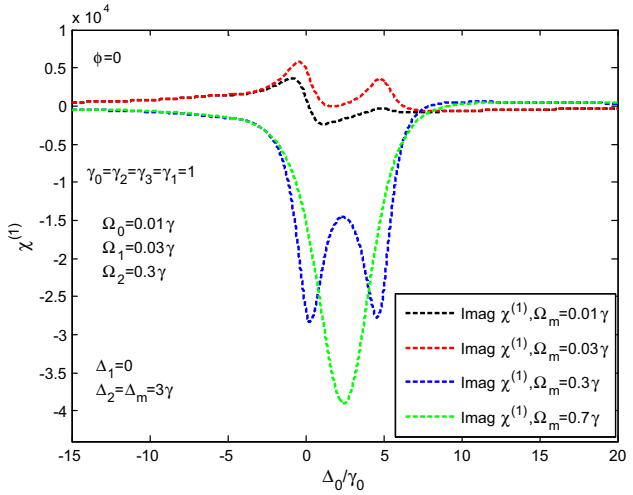

Figure 3. First-order susceptibility as a function of normalised probe detuning at different pumping fields Ω_m.

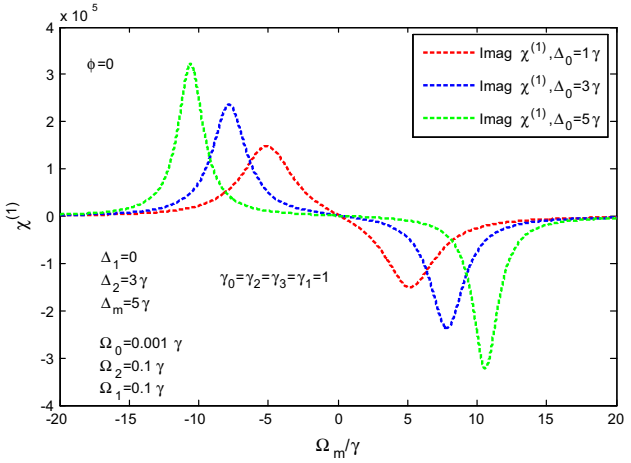

Figure 5. Linear susceptibility as a function of Rabi frequency of the pump field Ω_m.

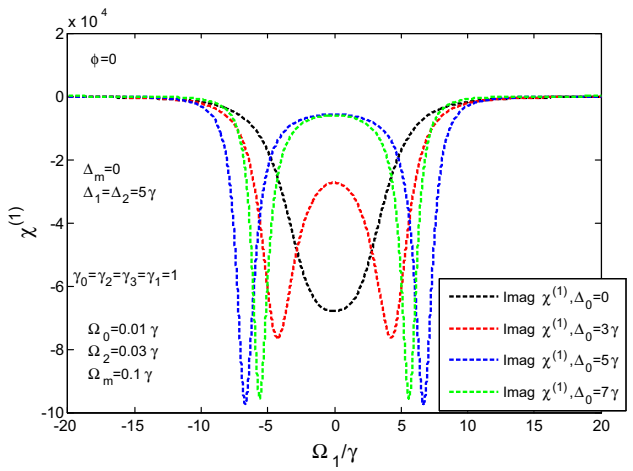

Figure 4. Linear susceptibility as a function of Rabi frequency of the cycling field Ω_1/γ at different probe detuning Δ_0.

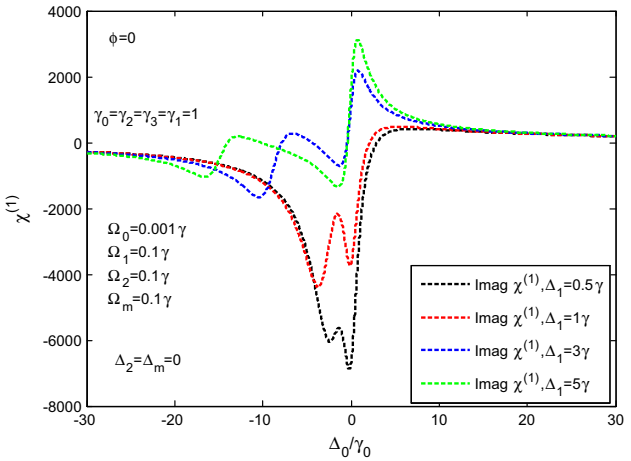

Figure 6. Linear susceptibility vs. the normalised probe detuning Δ_0/γ_0 under the effect of cycling detuning Δ_1.

the probe detuning. At the centre of the cycling field, the gain peak appears. When the system is probe-detuned, EIT was shown. Increasing probe detuning gives a wider EIT with a higher gain peak. Wide EIT is important in slow light applications [22]. Figure 5 shows linear susceptibility as a function of pumping field Ω_m with the probe detuning (Δ_0) as a variable parameter, where the detunings are: $\Delta_1 = 0$, $\Delta_2 = 3\gamma$ and $\Delta_m = 5\gamma$, while Rabi frequencies are $\Omega_0 = 0.01\gamma$ and $\Omega_1 = \Omega_2 = 0.1\gamma$. The behaviour under the effect of the pump field differs from that of the cycling field Ω_1 shown in figure 4, where the absorption peaks appear in the negative pump field frequencies and gain peaks appear in the positive pump field. So, one can use the pumping field to switch between absorption and gain. Both gain and absorption are increased and blue shifted with an increase in probe detuning.

Figure 6 shows the imaginary part of linear susceptibility vs. the normalised probe detuning. The following parameters are considered: the detunings are $\Delta_2 = \Delta_m = 0$, Rabi frequencies are $\Omega_0 = 0.001\gamma$ and $\Omega_1 = \Omega_2 = \Omega_2 = 0.1\gamma$, with the cycling field detuning Δ_1 as a parameter. At small cycling detuning $\Delta_1 = 0.5\gamma$ high gain (negative susceptibility) was obtained as in the black curve. Increase of cycling detuning to $\Delta_1 = \gamma$ (red curve) reduces the gain and an EIT window appears. More increment of cycle detuning $\Delta_1 = 3\gamma$ and 5γ fluctuates the susceptibility between absorption and gain at reduced values.

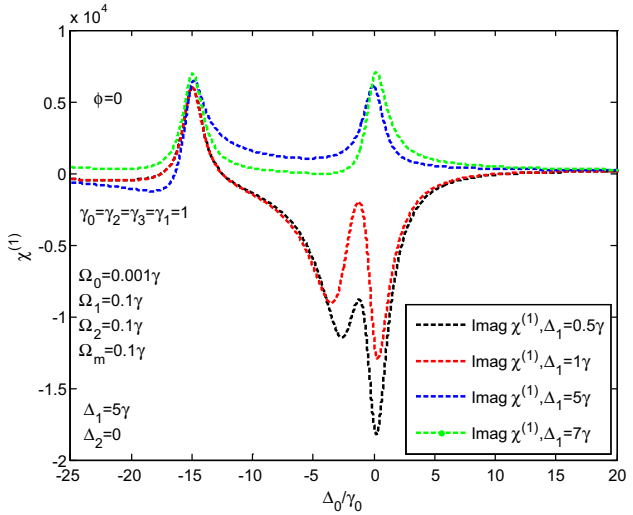

Figure 7. Linear susceptibility vs. Δ_0/γ_0 under the effect of cycling detunings.

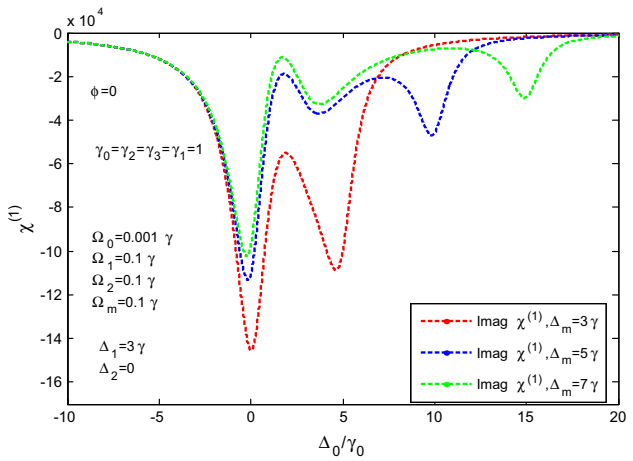

Figure 8. Linear susceptibility vs. the normalised probe detuning Δ_0/γ_0 at different pumping detuning Δ_m.

Figure 7 shows the same as in figure 6, but here while $\Delta_2 = 0$ increasing the pumping field to $\Delta_m = 5\gamma$ gives the gain (black and red curves) at $\Delta_1 = 0.5\gamma$ and γ and absorption at $\Delta_1 = 5\gamma$ and 7γ (blue and green curves), both with the wide EIT window obtained for absorption.

Figure 8 shows the effect of pump detuning (Δ_m) under $\Delta_1 = 3\gamma_1$, $\Delta_2 = 0$. A complete gain spectrum with the EIT window under different pump detunings ($\Delta_1 = 3\gamma, 5\gamma$ and 7γ) is obtained. A wide EIT window and reduction of gain were obtained at high pump detuning ($\Delta_m = 7\gamma$) as shown by the green curve.

Figure 9 shows the periodicity behaviour of linear susceptibility under the phase effect with the pumping field as a variable parameter. The gain with small amplitude was obtained at the low pump ($\Omega_m = 0.3\gamma$) as in the red

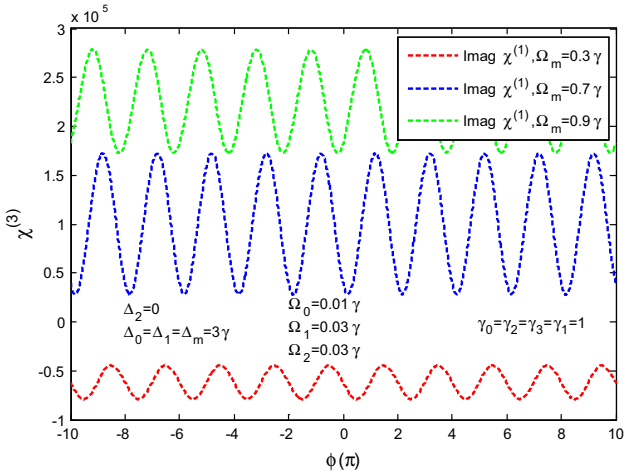

Figure 9. Linear susceptibility vs. the phase $\phi(\pi)$.

curve. The high pump ($\Omega_m = 0.7\gamma$) exhibits absorption with increased amplitude. More increments in the pump Rabi frequency reduce the absorption amplitude.

5. Conclusions

We discuss LWI in Y-configuration in a DQD nanostructure. It is found that changing the detuning of the spontaneous emission components of the cycling and pumping fields controls the laser emission. The results show that one can use the pumping field to switch between absorption and gain. Both gain and absorption are increased and blue shifted with the increase in probe detuning.

References

[1] B W Lovett, J H Reina, A Nazir, G Andrew and D Briggs, *Quantum Phys.* **8**, 1 (2008)
[2] B M Hutchins, T T Morgan, Mi G Ucak-Astarlioglu and M E Williams, *J. Chem. Educ*. **84**, 1301 (2007)
[3] A A Ukhanov, *Lasing without inversion*, http://info.phys.unm.edu/~ideutsch/Classes/Phys566F99/566_Journal/Articles/Ukhanov.pdf (1999)
[4] S E Harris, *Phys. Rev. Lett.* **62**, 1033 (1989)
[5] J Mompart, *J. Opt. B: Quantum Semiclass. Opt.* **2**, R7 (2000)
[6] M A Nielsen and I L Chuang, *Quantum computation and quantum information* (CUP, Cambridge, 2000) p. 2
[7] L F Cai, *Lasing without inversion in a closed four-level system*, arXiv:quant-ph/0512009 (2005)
[8] J Zou, D Xu and H Zhang, *Amplitude and phase control of gain without inversion in a four-level atomic system using loop-transition*, arXiv:1210.5817v2 (November 2013)

[9] K R Dastidar, L Adhya and R K Das, *Pramana – J. Phys.* **52**, 281 (1999)
[10] J M Villas-Boas, A O Govorov and S E Ulloa, *Phys. Rev. B* **6**, 125342 (2004)
[11] M Mahmoudi and M Sahrai, *Physica E* **41**, 1772 (2009)
[12] B Al-Nashy, S M M Amin and A H Al-Khursan, *J. Opt. Soc. Am. B* **125**, 4873 (2014)
[13] B Al-Nashy, S M M Ameen and A H Al-Khursan, *J. Opt.* **16**, 105205 (2014)
[14] G G Tarasov, Z Ya Zhuchenko, M P Lisitsa, Y I Mazur, Zh M Wang, G J Salamo, T Warming, D Bimberg and H Kissel, *Semiconductors* **40**, 79 (2006)
[15] A Vafafard, S Goharshenasan, N Nozari and A Mohmoudi, *J. Lumin.* **134**, 900 (2013)
[16] M Sahrai, M R Mehmannavaz and H Sattari, *Appl. Opt.* **53**, 2375 (2014)
[17] H R Hamedi, S H Asadpour and M Sahrai, *Optik* **124**, 366 (2013)
[18] X Yan, L Q Wang, B Y Yin and J P Song, *Optik* **122**, 986 (2011)
[19] A Joshi, *Phys. Rev. B* **79**, 115315 (2009)
[20] Y Jiang and K Zhu, arXiv:0801.3726v1 [cond-mat.mes-hall] **24**, 1 (2008)
[21] A H Al-Khursan, M K Al-Khakani and K H Al-Mossawi, *Photon. Nanostruct. Fundam. Appl.* **7**, 153 (2009)
[22] H Akram and A H Al-Khursan, *Appl. Opt.* **55**, 9866 (2016)